

Author's Accepted Manuscript

Polygodial analog induces apoptosis in LNCaP prostate cancer cells

Subramanyam Dasari, Angela Lincy Prem Antony Samy, Parnal Narvekar, Venkata Satish Dontaraju, Ramesh Dasari, Alexander Kornienko, Gnanasekar Munirathinam



PII: S0014-2999(18)30181-X
DOI: <https://doi.org/10.1016/j.ejphar.2018.03.029>
Reference: EJP71733

To appear in: *European Journal of Pharmacology*

Received date: 24 January 2018
Revised date: 13 March 2018
Accepted date: 15 March 2018

Cite this article as: Subramanyam Dasari, Angela Lincy Prem Antony Samy, Parnal Narvekar, Venkata Satish Dontaraju, Ramesh Dasari, Alexander Kornienko and Gnanasekar Munirathinam, Polygodial analog induces apoptosis in LNCaP prostate cancer cells, *European Journal of Pharmacology*, <https://doi.org/10.1016/j.ejphar.2018.03.029>

This is a PDF file of an unedited manuscript that has been accepted for publication. As a service to our customers we are providing this early version of the manuscript. The manuscript will undergo copyediting, typesetting, and review of the resulting galley proof before it is published in its final citable form. Please note that during the production process errors may be discovered which could affect the content, and all legal disclaimers that apply to the journal pertain.

Polygodial analog induces apoptosis in LNCaP prostate cancer cells

Subramanyam Dasari^{a1}, Angela Lincy Prem Antony Samy^{a1}, Parnal Narvekar^a, Venkata Satish Dontaraju^b, Ramesh Dasari^c, Alexander Kornienko^c, Gnanasekar Munirathinam^{a1*}

^aDepartment of Biomedical Sciences, College of Medicine, University of Illinois, Rockford, IL

^bInternal Medicine, Rockford Memorial Hospital, Rockford, IL

^cDepartment of Chemistry and Biochemistry, Texas State University, San Marcos, TX 78666

*Corresponding author. Dr. Gnanasekar Munirathinam, Department of Biomedical Sciences, University of Illinois College of Medicine, 1601 Parkview Avenue, Rockford, IL, 61107. Tel.: 815-395-5773. mgnanas@uic.edu

Abstract

Prostate cancer (PCa) is the second leading cause of death in American men. The chemotherapeutic treatment strategies are generally not effective and can lead to side effects. Hence, there is an urgent need to identify novel chemotherapeutic agents. The aim of this study was to synthesize and evaluate the therapeutic effects of a synthetic analog of polygodial (PG), a pungent constituent abundantly present in mountain pepper, water pepper and dorrigo pepper, on LNCaP PCa cell line and its anti-cancer mechanisms in a preclinical study. We evaluated the anti-cancer potential of the PG analog namely DRP-27 using various assays such as cell viability by MTT assay, anchorage independent growth by soft agar assay, reactive oxygen species generation by 2',7'-dichlorofluorescein probe-based fluorescence assay, and apoptosis by Annexin-V and TUNEL assays respectively. Western blot analysis was performed to identify the molecular mechanism of DRP-27-induced cell death. Our results showed that DRP-27 significantly inhibited LNCaP cell proliferation in a dose-dependent manner at 48 h treatment *in vitro*. In addition, DRP-27 potently inhibited anchorage-independent growth of these cells. Flow cytometry, Annexin-V and TUNEL assays confirmed that DRP-27 induces apoptosis in LNCaP cells. DRP-27 also induced the activation of intracellular reactive oxygen species. Western blot

¹ Contributed equally to the study

analysis revealed that DRP-27 downregulated the expression of survivin, while activating Bax and DNA damage marker pH₂AX in LNCaP cells. In conclusion, our study suggests that DRP-27 might be an effective anti-cancer agent for PCa.

Keywords: Prostate cancer, Polygodial, Reactive oxygen species, Apoptosis

1. Introduction

Prostate cancer (PCa) is the fourth most frequent neoplastic disease in general and the second most common cancer among men in western countries (Yoo et al., 2016). Approximately 1.1 million prostate cancer cases were diagnosed worldwide in 2012, accounting for 15% of all cancers in men (Ferlay et al., 2015) with the occurrence of 1 in 5 new diagnoses (Siegel et al., 2015). There are limited treatment options available for PCa. Patients with PCa is usually treated with surgery, chemotherapy (docetaxel and cabazitaxel) or secondary hormonal therapeutic agents (abiraterone or enzalutamide). Chemotherapy and radiation therapy are largely ineffective and metastatic disease invariably recurs in patients (Diaz and Patterson, 2004). However, the effects of these treatments are less satisfactory, and there is an urgent need for the development of effective novel anti-prostate cancer agents (Yoo et al., 2016).

Some of the traditional systems of medicine (Ayurveda and Unani) have used natural plant products for therapeutic purposes because they have many pharmacological effects with minimal side effects (Choudhury et al., 2010). Numerous studies have reported that certain compounds present in spices, such as black pepper, ginger, chilli, turmeric, possess anti-cancer properties (Brown et al., 2010; Choudhury et al., 2010; Sharma et al., 2005). One such natural compound is polygodial (PG), a pungent component of water pepper, dorrigo pepper and mountain pepper. It was originally isolated from the plant water pepper (*Polygonum hydropiper*) (Kubo et al., 2001). It is the most widely occurring sesquiterpene dialdehyde, having been found in flowering plants, ferns, liverworts, fungi, and marine molluscs from all around the world (Huq et al., 2014). PG is known to possess several pharmacological benefits such as antibacterial and antifungal, anti-allergic and anti-inflammatory properties. Its antifungal and antibacterial properties come from its ability to function as a non-ionic surfactant (Kubo et al., 2005; Montenegro et al., 2014). It has also been shown to inhibit mitochondrial ATPase, which can cause cell death of *Saccharomyces cerevisiae* (Lunde and Kubo, 2000). Previously, we reported

that a derivative of PG (9-epipolygodial, DRP-10) exhibits inhibitory activity against non-small cell lung cancer, melanoma, and glioma (Dasari et al., 2015b). We also reported that a Wittig derivative of PG (DRP-3) possesses promising activity against drug-resistant cancer cells. It was found to be effective against apoptosis-resistant cancer cells due to its cytostatic rather than cytotoxic effects (Dasari et al., 2015a). Based on the preliminary pharmacological evidence of anticancer activities of PG and its derivatives, we aimed to explore their anti-cancer effects on PCa cells. In this study, we designed a series of experiments to determine the effect of PG and its synthetic derivative DRP-27 on cell proliferation and anchorage-independent growth of androgen dependent PCa cell line (LNCaP). We also intended to identify the mechanism(s) by which DRP-27 exerts its anti-cancer effects in PCa cells.

2. Materials and Methods

2.1. Chemical synthesis

Compounds DRP-3 and DRP-10 were prepared as previously described (Dasari et al., 2015b, 2015a). Compound DRP-27 (diethyl ((E)-2-((1R,4aS,8aS)-1-formyl-5,5,8a-trimethyl-1,4,4a,5,6,7,8,8a-octahydronaphthalen-2yl)vinyl)phosphonate) was prepared by the following procedure: To a solution of tetraethyl methylenediphosphonate (36.9 mg, 0.128 mM) in THF (2 ml) was added *n*-BuLi (1.6 M) (80 μ l, 0.128 mM) at -78 °C and the mixture was stirred for 20 min. A solution of polygodial (10 mg, 0.0427 mM) in THF (1 ml) was then added dropwise at -78 °C. The resultant mixture was allowed to warm up to 0 °C and stirred for 2 h. After completion, the reaction was quenched with saturated NH₄Cl and then extracted with EtOAc. The organic layer was washed with water and dried over anhydrous Na₂SO₄ and then concentrated to give crude residue. The crude product was purified by preparative TLC using 60% EtOAc/hexanes solvent system to obtain DRP-27 in 95% yield (14.9 mg).

2.2. Characterization data:

¹H NMR (400 MHz, CDCl₃) δ 9.57 (d, J = 5.0 Hz, 1H), 9.47 (d, J = 4.8 Hz, 0.5H), 7.23 – 7.00 (m, 1.5H), 6.51 – 6.41 (m, 1.5H), 5.57 (t, J = 17.4 Hz, 1H), 5.26 (t, J = 17.1 Hz, 0.5H), 4.12 – 3.94 (m, 6H), 2.88 – 2.71 (m, 1.5H), 2.49 (dt, J = 20.2, 5.0 Hz, 1H), 2.31 (dt, J = 19.8, 4.8 Hz, 0.5H), 2.27 – 2.13 (m, 1.0H), 1.89 – 1.80 (m, 0.5H), 1.78 – 1.64 (m, 3H), 1.63 – 1.55 (m, 1.5H), 1.54 – 1.45 (m, 3H), 1.35 – 1.25 (m, 9H), 1.23 – 1.14 (m, 3H), 1.02 – 0.87 (m, 13.5H); ¹³C NMR

(100 MHz, CDCl₃) δ 205.4, 201.7, 150.6, 150.5, 150.0, 149.9, 141.2, 141.2, 141.0, 140.9, 130.9, 130.7, 129.3, 129.0, 113.13, 113.1, 111.25, 111.23, 62.61, 62.60, 62.15, 62.14, 61.5 (m) 60.4, 48.6, 44.6, 42.1, 41.8, 40.2, 37.7, 37.4, 36.6, 33.2, 33.1, 32.7, 25.37, 25.36, 24.7, 24.7, 22.2, 21.9, 21.2, 21.0, 18.4, 18.0, 16.36 (m), 15.5, 14.2; HRMS m/z (ESI) calcd for C₂₀H₃₄O₄P (M+H⁺) 369.2195, found 369.2193.

2.3. Prostate cancer cell lines

LNCaP, PC-3, DU145 and RWPE-1 cells were obtained from ATCC. PCa cell lines (LNCaP, PC-3 and DU145) were cultured in RPMI-1640 (Lonza) media supplemented with 10% (v/v) fetal bovine serum (FBS), 1% (v/v) antimycotic and 0.6% (v/v) antibiotic (Sigma Aldrich) at 37°C and 5% CO₂. RWPE-1 cells were cultured in KSFM media (Gibco) supplemented with bovine pituitary extract (25µg/ml) and EGF (5ng/ml) at 37°C in 5% CO₂ environment. Polygodial (PG) was obtained from Sigma. All drugs were dissolved in dimethyl sulfoxide (DMSO), purchased from Fisher Biotech, to make 10 mM stock. Further dilutions were made in plain RPMI-1640 media.

2.4. Cell viability assay by MTT

To study the effects of PG and its derivatives on cell viability, PCa cells (LNCaP, PC-3 and DU-145) were treated with PG and its derivatives. Cell viability was determined by measuring 3-(4,5-dimethylthiazol-2-yl)-2,5-diphenyltetrazolium bromide (MTT) (Sigma) colorimetric dye reduction (van Meerloo et al., 2011). PCa cells were cultured in 96-well plates at a cell density of 1x10³/well in complete RPMI-1650 (10% FBS, 1% antimycotic and 0.6% antibiotic) and allowed to incubate at 37°C in 5% CO₂ environment. The cells were treated with various concentrations (0, 2.5, 5, 10 and 20 µM) of PG and its derivatives for 48 h. 10 µl of MTT reagent (5 mg/ml) was added to each well and the plates were incubated for 3 h at 37 °C and the crystals were dissolved by using a solubilization solution. The absorbance was measured at 570 nm using Bio-Rad plate reader. The percentage of cell viability was determined relative to the control. Each treatment dosage was performed in replicates of six and was repeated three times to obtain consistent results. To evaluate the anti-cancer mechanism of DRP-27, LNCaP cells were treated in combination of DRP-27 and caspase inhibitor (CI) (Z-VAD-FMK), antioxidant N-acetyl cysteine (NAC) or autophagy inhibitor 3-methyladenine (3-MA). Similarly, the cytotoxicity of

DRP-27 was evaluated on normal prostate cells (RWPE-1). The RWPE-1 cells were seeded, treated with various concentrations of DRP-27 and evaluated for cell viability as described above.

2.5. Anchorage-independent colony formation assay

Colony formation or soft agar assay was performed to evaluate the effects of PG derivative (DRP-27) on anchorage-independent growth of PCa cells as described previously (Franken et al., 2006). LNCaP cells ($15\text{-}20 \times 10^3$) were mixed with 0.7% agarose (ISC Bioexpress) solution in complete RPMI with 20% FBS and poured on top of solidified 1% base agar (Thermofisher) in 6-well plates. Various concentration of PG and its derivatives were also mixed with soft agarose and allowed to incubate for 4-5 weeks. Cells were fed with complete RPMI containing 20% FBS every 4 days for up to 4 weeks. After the incubation period the colonies were stained with 0.005% crystal violet and examined with a microscope.

2.6. Measurement of reactive oxygen species

The relative levels of cellular peroxides induced by DRP-27 were determined using reactive oxygen species fluorescent probe, 2',7'-dichlorofluorescein diacetate (DCFDA). LNCaP cells (2×10^4 cells/500 μ l) were cultured in 8-chamber tissue culture slide and treated with various concentrations of DRP-27 (0, 5, 10 and 20 μ M), incubated at 37 °C, 5% CO₂ for 48 h. Cells were then washed with PBS and incubated with 10 μ M DCFDA dye suspended in serum-free medium for 30 min at 37 °C. The green fluorescence was detected using a microscope (Olympus). The intensity of fluorescence was quantified using ImageJ software (v.1.4.3.67).

2.7. Assessment of apoptosis in LNCaP cells by flow cytometry.

Apoptosis in LNCaP cells after treatment with DRP-27 was determined using flow cytometry as described previously with some minor modifications (Thirugnanam et al., 2008). In brief, LNCaP cells (6×10^5) were treated with DRP-27 for 48 h, detached and attached cells were collected and washed twice with ice-cold PBS. The collected cells were then re-suspended in 500

μl of 1X binding buffer, 5 μl Annexin V-FITC and 5 μl of propidium iodide were added and incubated for 15 min at room temperature in the dark. The number of apoptotic cells were quantified by flow cytometer (Becton Dickinson, USA) and data analyzed by CellQuest software.

2.8. Detection of Apoptosis by Annexin V-FITC Staining

Apoptotic cell death was detected by Annexin V-FITC kit (BioVision Inc). For this experiment, 2×10^4 cells/500 μl of complete RPMI-1640 were cultured in 8-chamber tissue culture slide and treated with various concentrations of DRP-27 (0, 5, 10 and 20 μM). After 48 h, cells were stained with 5 μl of Annexin-V-FITC and 5 μl of PI, dissolved in 500 μl of binding buffer per well, and incubated in the dark at room temperature for 10 min. The cells were washed and analyzed for the apoptotic cell morphology under a fluorescence microscope.

2.9. Detection of Apoptosis by TUNEL Assay

The TUNEL assay was performed to visualize the apoptotic cell death using an *in-situ* cell death detection kit (AAT Bioquest, Inc. CA, USA). The protocol was followed according to the manufacturer's guidelines. The LNCaP cells were grown in a 96-well plate, treated with various concentrations of DRP-27 and incubated for 48 h at 37 °C and 5% CO₂. After treatment, cells were washed and fixed (4% paraformaldehyde) for 30 min at room temperature. Samples were incubated with 50 μl of TUNEL reagent (TdT-mediated digoxigenin-dUTP nick-end labeling) provided in the kit for 1 h at 37°C in a dark chamber. Samples were washed with PBS and mixed with the Hoechst stain (30 nM) for 5 min. TUNEL fluorescence was visualized with an Olympus fluorescence microscope (Culture Microscopes, Olympus, Center Valley, PA, USA).

2.10. Assessment of active caspase-3

The active caspase-3 level was measured using quantitative caspase-3 ELISA kit (R&D Systems, Inc. USA). Cells were treated with various concentrations of DRP-27 and vehicle alone (control group) for 48 h. After incubation, cell extracts were prepared according to manufacturer instructions. Briefly, cells were mixed with the lysis buffer and cell lysates were transferred into the wells of a microplate, pre-coated with a monoclonal antibody specific for caspase-3. Following this, substrate solution (streptavidin-HRP) was added to the wells. The enzyme

reaction yielded a blue product that turned yellow when a stop solution was added. The optical density of each well was determined within 30 min, using a microplate reader (Synergy 2 Multi-Mode Reader, BioTeK, Winooski, Vermont, USA) set to 450 nm with a wavelength correction at 540 nm or 570 nm. The active caspase-3 concentrations were calculated from a standard curve constructed using known concentrations of active caspase-3.

2.11. Nuclear morphology detection by Hoechst 33258

Hoechst 33258 was employed to label both intact and apoptotic nuclei (Durand and Olive, 1982; Jiang et al., 2014). Cells were seeded in 96-well plates at a density of 1×10^5 cells/well, followed by DRP-27 treatment (10 μ M). Following treatment, the LNCaP cells were washed in ice-cold PBS buffer (pH 7.4), fixed with 4% p-formaldehyde and incubated with 1 μ g/ml Hoechst 33258 for 3-5 min at room temperature. Condensed and fragmented nuclei were evaluated using fluorescent probe Hoechst 33258. Visualization was conducted at an excitation and emission wavelengths of 480 and 520 nm, respectively, by Olympus IMT-2 fluorescence microscopy (Tokyo, Japan).

2.12. Detection of phosphoH₂AX and cleaved caspase-3 by confocal immunofluorescence

LNCaP cells were cultured in 8-chamber plates, treated with DRP-27 (10 μ M) and incubated at 37 °C and 5% CO₂ for 48 h. Cells were fixed (4% formaldehyde) for 15 min and blocked with 5% goat normal serum (Invitrogen) with 0.3% Triton X- 100 (Sigma–Aldrich) in PBS. Cells were washed (PBS) and incubated with primary antibodies (1:200) (pH2AX and cleaved caspase-3) for 1 h. After three successive washings, cells were treated with either 0.1 μ g/ml of anti-mouse IgG or secondary anti-rabbit IgG conjugated with FITC for 1 h. Cells were counter stained with DAPI (30 nm) for 10-20 min, washed with PBS and a coverslip with Fluorogel (Electron Microscopy Sciences, Hatfield, PA, USA) was prepared for visual inspection with an Olympus FluoView confocal microscope. The quantification of the image was done using ImageJ software.

2.13. Protein expression profiling using Western blot analysis

DRP-27 treated cells were harvested using cell scrappers and washed with serum free medium. Total cellular protein was isolated using lysis buffer (BD Pharmingen) (Liu et al., 2014). Protein concentration was determined using a protein assay kit (Pierce chemicals, USA). Equal amounts

of protein with Laemmli sample buffer (Bio-Rad) were loaded in each lane, separated using 12% SDS-PAGE and transferred to nitro cellulose membranes by semi-dry transfer method. The membranes were blocked with 5% skim milk in Tris Buffered Saline (TBS) and incubated with primary antibodies (1:1000). After washing with TBS-Tween-20, the membranes were incubated with corresponding peroxidase-conjugated goat anti-mouse or anti-rabbit secondary antibodies followed by detection with enhanced chemiluminescence staining and the bands were observed on an X-ray film. β -Actin/GAPDH was used to normalize protein loading. The expression level of protein was quantified by ImageJ software (v1.4.3.67) analysis (Kaur and Bachhawat, 2009).

2.14. Statistical analysis

Statistical analysis was performed using Student's t-test. The differences were considered statistically significant when $P < 0.05$.

3.0 Results

3.1. Synthesis of polygodial derivatives

The preparation of compounds used in the current study is shown in Figure 1. DRP-10 was obtained from PG by acid-catalyzed epimerization at C9 position, which is alpha to the C11-aldehyde moiety (Fig. 1). This reaction leads to a thermodynamic mixture, from which the desired compound DRP-10 can be isolated in 40% yield. To obtain DRP-3, PG was reacted with a stabilized Wittig reagent highly selectively at the C12-aldehyde group (Fig. 1). It appears that the C11-aldehyde is sterically shielded by the adjacent quaternary center. DRP-3 was produced in a high 94% yield. Finally, PG was reacted with tetraethyl methylene bisphosphonate to produce DRP-27 in an excellent 95% yield (Fig. 1). Although the reaction proceeded highly selectively at the C12-aldehyde, the position C9, alpha to the C11-aldehyde moiety, underwent epimerization under the highly basic reaction conditions. Unfortunately, our attempts to separate the epimers were futile. Thus, compound DRP-27 represents a mixture of two epimers at C9.

3.2. Anti-cancer effects of PG and its derivatives

PG and its derivatives (DRP-3, DRP-10 and DRP-27) inhibit the growth of LNCaP cells. Of the compounds tested, DRP-27 showed robust inhibition of LNCaP growth with the IC_{50} value of 5 μ M (Fig. 2A). We observed that anti-proliferative effects of DRP-27 were significantly

abrogated in presence of anti-oxidant N-acetyl cysteine (NAC) and caspase inhibitor (Z-VAD-FMK) suggesting that the reactive oxygen species and caspase activation are the underlying mechanisms of DRP-27 effects on LNCaP cells (Fig. 2B). The DRP-27 treatment also induced marked morphological changes, including cytoplasmic shrinkage and cellular flattening following the 48 h treatment (Fig. 2C). We also evaluated the cytotoxicity of DRP-27 on PC-3, DU145 and normal prostate cells (RWPE-1), in which DRP-27 does not exhibit significant cytotoxicity even at higher concentration (28% of cell viability inhibition at 50 μ M) (Fig. 2D). Of all these cells tested, LNCaP displayed higher sensitivity to DRP-27 compared to DU145 or PC-3. Therefore, further experiments were performed using LNCaP cells. Results showed that DRP-27 significantly inhibited the anchorage-independent growth (*in vitro* tumorigenesis) of LNCaP cells. Untreated cells grew in large colonies, whereas no colonies were observed in the DRP-27-treated cells (Fig. 2E). These results suggest that DRP-27 has the potential to inhibit prostate tumor growth.

3.3. DRP-27 induces reactive oxygen species generation and apoptotic cell death in LNCaP cells

When LNCaP cells were treated with DRP-27, the induction of reactive oxygen species could be observed using immunofluorescent probe (DCFDA). Fig. 3A illustrates a significant induction of reactive oxygen species production in DRP-27 treated LNCaP cells compared with the untreated cells. The well-known antioxidant N-acetyl cysteine (NAC), abrogated the effect of DRP-27 by decreasing the reactive oxygen species production (Fig. 3A) suggesting that oxidative stress as the potential mechanism of cytotoxicity of DRP-27 in LNCaP cells. A quantitative analysis of reactive oxygen species production was performed by measuring the DCFDA fluorescence intensity with ImageJ software (Fig. 3B). Significant differences (* $P < 0.01$) were observed between control and DRP-27 treatment groups and (# $P < 0.01$) between DRP-27 alone and NAC + DRP-27 treatments. DRP-27 induced internucleosomal DNA fragmentation, which is associated with chromatin condensation was observed by Hoechst 33258 staining using inverted fluorescence microscopy. As shown in Fig. 3D, DRP-27 led to condensed and fragmented nuclei compared with the control, indicating possible apoptosis activation by DRP-27 in LNCaP cells. To investigate whether apoptosis was triggered by DRP-27 treatment, LNCaP cells were analyzed by Annexin V FITC/PI flow cytometry. Significant number of apoptotic cells were

detected in LNCaP cells treated with DRP-27 (10 and 20 μ M) when compared with untreated cells (Fig. 3E).

3.4. DRP-27 induces apoptotic cell death via caspase-3 activation

To further investigate the effects of DRP-27 on apoptosis induction, LNCaP cells were treated with various concentrations of (0, 10 and 20 μ M) DRP-27 for 48 h. As shown in Fig. 4A, we found that DRP-27 induced apoptosis in LNCaP cells as these cells were positive for Annexin V-FITC (green color) and propidium iodide (red color). DRP-27-induced apoptosis was further confirmed by terminal nucleotidyl transferase-mediated nick end labeling (TUNEL) assay. Indeed, we found that DRP-27 induced a dose dependent increase in the apoptosis of LNCaP cells compared to control cells (Fig. 4A). Quantitative analysis of color intensity produced by TUNEL stain (red) and Hoechst 33342 stain (blue) was determined by ImageJ software (Fig. 4B). Caspase-3 is the key executioner of apoptotic process in cancer cells. Therefore, we quantified the levels of cleaved caspase-3 following DRP-27 treatment in LNCaP cells using quantitative ELISA method. Figure 4D, shows that at 20 μ M concentration, DRP-27 induces significant ($P < 0.01$) increase in active caspase-3 when compared to control cells. In addition to ELISA, Western blot results (Fig. 4E) showed that procaspase-3 levels were decreased indicating potential caspase-3 activation. Caspase-3 cleavage in DRP-27 treated LNCaP cells was analyzed using confocal analysis. Results of confocal immunohistochemistry (Fig. 4F and 4G) showed that DRP-27 promotes caspase-3 cleavage suggesting that DRP-27 induces apoptosis via caspase-3 activation.

3.5. DRP-27 induces DNA damage response by p H_2 AX

The DNA damage response was measured by the levels of phosphorylated histone H_2 AX (p H_2 AX). Immunofluorescence analysis of p H_2 AX labeled with FITC (green color) indicated the increased levels of p H_2 AX in DRP-27-treated LNCaP cells compared to untreated LNCaP cells (Fig. 5A). Increased p H_2 AX (FITC-green color) expression as quantified by Image-J software (Fig. 5B) analysis suggested that DRP-27 induced DNA damage response in LNCaP cells. The

DNA damage response can be measured by double-stranded breaks (DSBs), which rapidly result in the phosphorylation of histone H₂AX (Sharma et al., 2012).

3.6. Protein expression profiling using Western blot analysis

DRP-27-induced apoptosis was confirmed by the cleavage of PARP-1, a substrate for caspase-3 using Western blot. As shown in Fig. 6, the cleavage of PARP-1 in LNCaP cells was detectable at 10 μ M DRP-27 by the appearance of 89 KDa cleaved product. As evidence that DRP-27 induces DNA damage, we also examined the activation of p γ H2AX. Western blot analysis of cell lysates showed robust induction of p γ H2AX in LNCaP cells treated with DRP-27. DRP-27 also down regulated the expression of Survivin, an inhibitor of apoptosis (IAP) family with concurrent activation of pro-apoptotic protein, Bax. The survivin protein functions to inhibit caspase activation, thereby leading to negative regulation of apoptosis or programmed cell death (Mita et al., 2008).

4.0 Discussion

Previous studies suggest that certain compounds extracted from spices such as ginger, black pepper, turmeric and chilies possess anti-cancer properties (Brown et al., 2010; Choudhury et al., 2010; Sharma et al., 2005). One such compound is polygodial (PG), the active compound of pepper seeds (Dorrigo pepper, mountain pepper and water pepper). Chemically, PG is a sesquiterpene dialdehyde and is known to possess anti-bacterial, anti-fungal, anti-hyperalgesic and anti-inflammatory activities (Kubo et al., 2001, 2005). In this study, we evaluated the anti-cancer activity of a new PG derivative, DRP-27 against androgen sensitive human prostate cancer cells (LNCaP). Cell viability analysis of PG and its derivatives indicated that PG derivatives showed more pronounced anti-proliferative activity than the parent PG, with DRP-27 being the most potent. Combinational treatment shows that antioxidant N-acetyl cysteine (NAC), caspase inhibitor (CI), Z-VAD-FMK significantly abrogated, and autophagy inhibitor 3-MA partially abrogated the effects of DRP-27, suggesting that reactive oxygen species and caspase activation are the potential underlying anti-cancer mechanisms of DRP-27 in LNCaP cells. We also evaluated the cytotoxicity of the DRP-27 on normal prostate cells. Of note, there is no significant cytotoxic effect of DRP-27 on benign prostate cells (RWPE-1 cells) suggesting its specific effect on LNCaP cells. Loss of contact inhibition and anchorage-independent growth are

characteristics of tumor cells (Wang, 2004). Therefore, agents that target these malignant properties of cancer cells could be potential treatment for cancer. Anti-clonogenic potential of DRP-27 was studied using soft agar assay. Recent studies have reported that piperine, a major component of pepper, inhibits colony formation in human colon cancer cells (HT-29) and osteosarcoma cells (HOS and U₂OS), in a dose depended manner (Yaffe et al., 2015; Zhang et al., 2015). Similarly, in the present study, DRP-27 treatment reduced the size and number of colonies in LNCaP cells in a dose dependent manner compared with the control cells. Thus, DRP-27 inhibits the anchorage independent property of androgen dependent PCa cells (LNCaP cells), thereby indicating its potential anti-tumorigenic activity. It is well established that reactive oxygen species are known mediators of intracellular cascade signaling for most of the cellular death mechanisms. The excessive generation of reactive oxygen species induces damages to the biomolecules and induces oxidative stress, loss of cell functionality and apoptosis (Slater et al., 1995). Since NAC abrogated the effects of DRP-27, we postulate that DRP-27 may increase the levels of reactive oxygen species, which could be involved in apoptosis. In our study, the levels of reactive oxygen species were significantly increased in a dose dependent manner in DRP-27 treated cells compared to control cells. Our results indicated that reactive oxygen species generation was effectively diminished by pretreatment with reactive oxygen species scavengers (NAC) when cells were treated with DRP-27. Therefore, the intracellular reactive oxygen species appears to be critical for its anti-cancer mechanisms in DRP-27-induced cell death in LNCaP cells, because oxidative stress is implicated in many biological processes such as cell cycle arrest, DNA damage and apoptosis (Rasul et al., 2013).

The chemical nature of polygodial is sesquiterpene, a plant derived compound used for various health conditions such as thyroiditis, asthma, allergies, arthritis, and autoimmune diseases (Barrosa et al., 2016). Sesquiterpene lactones (SLs) compounds can induce apoptosis of cancer cell by decreasing the levels of intracellular reduced glutathione (GSH). Treatment of SL can affect intracellular redox signaling pathways that are directly involved in the apoptosis mechanism (Gach et al., 2015). It is well established that SL-induced apoptosis is associated with increased generation of reactive oxygen species, decreased mitochondrial transmembrane potential, glutathione (GSH) depletion, cytochrome c release, and activation of caspases (caspase 3, 9 and 7) (Khan et al., 2012; Wen et al., 2002). Mitochondria is an important component of the apoptosis execution machinery, which involves pro-apoptotic events including decreased

mitochondrial membrane potential ($\Delta\psi_m$), release of cytochrome C and activation of caspase cascade (Elmore, 2007). It is becoming increasingly apparent that the mitochondria play a fundamental role in the processes leading to cell death (Wang and Youle, 2009). Previously, Lunde and Kubo, (2000) reported that plasma membrane disruption is the mechanism of polygodial-induced cell death. Specifically, polygodial inhibits the mitochondrial ATPase in a dose-dependent manner at fungicidal concentration (Lunde and Kubo, 2000). Therefore, we speculate that DRP-27 could target mitochondria in prostate cancer cells to execute apoptosis, which needs further evaluation.

Apoptosis is a programmed cell death characterized by specific morphological and energy-dependent biochemical mechanism (Elmore, 2007). Accumulated evidences suggest that most of the chemotherapeutic agents halt tumor cell growth and proliferation through induction of apoptosis (Rasul et al., 2013). In this study, we examined whether DRP-27 inhibited growth of PCa (LNCaP) cells through the induction of apoptosis. DRP-27-induced apoptosis was determined by flow cytometry, Annexin-V binding, and TUNEL assays. The results of these assays suggest that 10 μ M concentration of DRP-27 was sufficient to induce potent apoptosis in LNCaP cells. We also found that pre-treatment with NAC completely blocked the apoptotic effect of DRP-27 indicating that induction of apoptosis is reactive oxygen species-dependent. Further, we confirmed the activation of caspase-3 and PARP-1 cleavage in DRP-27 treated LNCaP cells. Activation of Poly(ADP-ribose) polymerase-1 (PARP-1) is involved in cellular response to DNA damage (Cepeda et al., 2006). In the present study, DRP-27 promoted the cleavage of PARP-1, indicating that DRP-27 induces DNA damage response in LNCaP cells. Phosphorylation of the subtype of histone H₂A, specifically H₂AX (γ H₂AX), is another important cellular response to DNA damage involving either cell cycle arrest or apoptosis (Podhorecka et al., 2010). We observed that DRP-27 elevated the levels of γ H₂AX in LNCaP, which is confirmed by immunofluorescence of γ H₂AX and western blot analysis. The caspases are a class of proteins associated with apoptotic process via activation of the death receptors and mitochondrial pathways to accomplish the programmed cell death (Cohen, 1997). Caspases are present in the form of inactive zymogens, which are activated during process of apoptosis. Among these, caspase-3 is an important and frequently activated protease, catalyzing the specific cleavage of many key cellular proteins including PARP-1 (Adams, 2003; Porter and Jänicke, 1999). The results showed that procaspase-3 was cleaved to yield two fragments (17 and 20

KDa). We further confirmed caspase-3 activation using ELISA, showing that 5 μ M concentration of DRP-27 is sufficient to activate caspase-3 compared to control. These findings are consistent with previous studies, showing that sesquiterpene lactones (e.g., 9 β -acetoxycostunolide) induce the apoptosis by the activation of caspase-3 (Ma et al., 2009).

Conclusion

In summary, the analog of PG (DRP-27) may be an effective anti-cancer agent for PCa. Based on our *in vitro* studies with LNCaP cells, DRP-27 specifically induces reactive oxygen species-mediated apoptotic cell death (Fig. 7). As follow up to these *in vitro* results, further studies are needed to evaluate the therapeutic potential of DRP-27 against PCa in experimental *in vivo* models.

Acknowledgement

Authors would like to thank the Department of Biomedical Science, University of Illinois, Rockford for supporting this study. This study is also partly supported by funding received from NIH, United States (R21 CA184646-01A1 and R03 CA212890-01A1) and Brovember Inc. Rockford.

Competing Interest Statement

Authors declare that they do not have conflict of interest.

Author contributions

SD, ALPAS, PN, and RD performed the experiments. SD, ALPAS, SVD, AK, and GM analyzed and interpreted the data. SD, ALPAS, SVD, AK and GM wrote the paper.

References

- Adams, J.M., 2003. Ways of dying: multiple pathways to apoptosis. *Genes Dev.* 17, 2481–2495. <https://doi.org/10.1101/gad.1126903>
- Barrosa, K.H., Mecchi, M.C., Rando, D.G., Ferreira, A.J.S., Sartorelli, P., Valle, M.M.R., Bordin, S., Caperuto, L.C., Lago, J.H.G., Lellis-Santos, C., 2016. Polygodial, a sesquiterpene isolated from *Drimys brasiliensis* (Winteraceae), triggers glucocorticoid-like effects on pancreatic β -cells. *Chem. Biol. Interact.* 258, 245–256. <https://doi.org/10.1016/j.cbi.2016.09.013>

- Brown, K.C., Witte, T.R., Hardman, W.E., Luo, H., Chen, Y.C., Carpenter, A.B., Lau, J.K., Dasgupta, P., 2010. Capsaicin displays anti-proliferative activity against human small cell lung cancer in cell culture and nude mice models via the E2F pathway. *PLoS One* 5, e10243. <https://doi.org/10.1371/journal.pone.0010243>
- Cepeda, V., Fuertes, M.A., Castilla, J., Alonso, C., Quevedo, C., Soto, M., Pérez, J.M., 2006. Poly(ADP-ribose) polymerase-1 (PARP-1) inhibitors in cancer chemotherapy. *Recent Patents Anticancer Drug Discov.* 1, 39–53.
- Choudhury, D., Das, A., Bhattacharya, A., Chakrabarti, G., 2010. Aqueous extract of ginger shows antiproliferative activity through disruption of microtubule network of cancer cells. *Food Chem. Toxicol. Int. J. Publ. Br. Ind. Biol. Res. Assoc.* 48, 2872–2880. <https://doi.org/10.1016/j.fct.2010.07.020>
- Cohen, G.M., 1997. Caspases: the executioners of apoptosis. *Biochem. J.* 326 (Pt 1), 1–16.
- Dasari, R., De Carvalho, A., Medellin, D.C., Middleton, K.N., Hague, F., Volmar, M.N.M., Frolova, L.V., Rossato, M.F., De La Chapa, J.J., Dybdal-Hargreaves, N.F., Pillai, A., Kälin, R.E., Mathieu, V., Rogelj, S., Gonzales, C.B., Calixto, J.B., Evidente, A., Gautier, M., Munirathinam, G., Glass, R., Burth, P., Pelly, S.C., van Otterlo, W.A.L., Kiss, R., Kornienko, A., 2015a. Wittig derivatization of sesquiterpenoid polygodial leads to cytostatic agents with activity against drug resistant cancer cells and capable of pyrrolylation of primary amines. *Eur. J. Med. Chem.* 103, 226–237. <https://doi.org/10.1016/j.ejmech.2015.08.047>
- Dasari, R., De Carvalho, A., Medellin, D.C., Middleton, K.N., Hague, F., Volmar, M.N.M., Frolova, L.V., Rossato, M.F., De La Chapa, J.J., Dybdal-Hargreaves, N.F., Pillai, A., Mathieu, V., Rogelj, S., Gonzales, C.B., Calixto, J.B., Evidente, A., Gautier, M., Munirathinam, G., Glass, R., Burth, P., Pelly, S.C., van Otterlo, W.A.L., Kiss, R., Kornienko, A., 2015b. Synthetic and Biological Studies of Sesquiterpene Polygodial: Activity of 9-Epipolygodial against Drug-Resistant Cancer Cells. *ChemMedChem* 10, 2014–2026. <https://doi.org/10.1002/cmdc.201500360>
- Diaz, M., Patterson, S.G., 2004. Management of androgen-independent prostate cancer. *Cancer Control J. Moffitt Cancer Cent.* 11, 364–373.
- Durand, R.E., Olive, P.L., 1982. Cytotoxicity, Mutagenicity and DNA damage by Hoechst 33342. *J. Histochem. Cytochem. Off. J. Histochem. Soc.* 30, 111–116. <https://doi.org/10.1177/30.2.7061816>
- Elmore, S., 2007. Apoptosis: a review of programmed cell death. *Toxicol. Pathol.* 35, 495–516. <https://doi.org/10.1080/01926230701320337>
- Ferlay, J., Soerjomataram, I., Dikshit, R., Eser, S., Mathers, C., Rebelo, M., Parkin, D.M., Forman, D., Bray, F., 2015. Cancer incidence and mortality worldwide: sources, methods and major patterns in GLOBOCAN 2012. *Int. J. Cancer* 136, E359–386. <https://doi.org/10.1002/ijc.29210>
- Franken, N.A.P., Rodermond, H.M., Stap, J., Haveman, J., van Bree, C., 2006. Clonogenic assay of cells in vitro. *Nat. Protoc.* 1, 2315–2319. <https://doi.org/10.1038/nprot.2006.339>
- Gach, K., Długosz, A., Janecka, A., 2015. The role of oxidative stress in anticancer activity of sesquiterpene lactones. *Naunyn. Schmiedebergs Arch. Pharmacol.* 388, 477–486. <https://doi.org/10.1007/s00210-015-1096-3>
- Huq, A.K.M.M., Jamal, J.A., Stanslas, J., 2014. Ethnobotanical, Phytochemical, Pharmacological, and Toxicological Aspects of *Persicaria hydropiper* (L.) Delarbre. *Evid.-Based Complement. Altern. Med. ECAM* 2014, 782830. <https://doi.org/10.1155/2014/782830>
- Jiang, H., Li, J., Zhou, T., Wang, C., Zhang, H., Wang, H., 2014. Colistin-induced apoptosis in PC12 cells: Involvement of the mitochondrial apoptotic and death receptor pathways. *Int. J. Mol. Med.* 33, 1298–1304.

- Kaur, J., Bachhawat, A.K., 2009. A modified Western blot protocol for enhanced sensitivity in the detection of a membrane protein. *Anal. Biochem.* 384, 348–349.
<https://doi.org/10.1016/j.ab.2008.10.005>
- Khan, M., Yi, F., Rasul, A., Li, T., Wang, N., Gao, H., Gao, R., Ma, T., 2012. Alantolactone induces apoptosis in glioblastoma cells via GSH depletion, ROS generation, and mitochondrial dysfunction. *IUBMB Life* 64, 783–794. <https://doi.org/10.1002/iub.1068>
- Kubo, I., Fujita, K., Lee, S.H., 2001. Antifungal mechanism of polygodial. *J. Agric. Food Chem.* 49, 1607–1611.
- Kubo, I., Fujita, K., Lee, S.H., Ha, T.J., 2005. Antibacterial activity of polygodial. *Phytother. Res. PTR* 19, 1013–1017. <https://doi.org/10.1002/ptr.1777>
- Liu, Z.-Q., Mahmood, T., Yang, P.-C., 2014. Western blot: technique, theory and trouble shooting. *North Am. J. Med. Sci.* 6, 160. <https://doi.org/10.4103/1947-2714.128482>
- Lunde, C.S., Kubo, I., 2000. Effect of polygodial on the mitochondrial ATPase of *Saccharomyces cerevisiae*. *Antimicrob. Agents Chemother.* 44, 1943–1953.
- Ma, G., Chong, L., Li, Z., Cheung, A.H.T., Tattersall, M.H.N., 2009. Anticancer activities of sesquiterpene lactones from *Cyathocline purpurea* in vitro. *Cancer Chemother. Pharmacol.* 64, 143–152.
<https://doi.org/10.1007/s00280-008-0863-y>
- Mita, A.C., Mita, M.M., Nawrocki, S.T., Giles, F.J., 2008. Survivin: Key Regulator of Mitosis and Apoptosis and Novel Target for Cancer Therapeutics. *Clin. Cancer Res.* 14, 5000–5005.
<https://doi.org/10.1158/1078-0432.CCR-08-0746>
- Montenegro, I., Tomasoni, G., Bosio, C., Quiñones, N., Madrid, A., Carrasco, H., Olea, A., Martinez, R., Cuellar, M., Villena, J., 2014. Study on the cytotoxic activity of drimane sesquiterpenes and nordrimane compounds against cancer cell lines. *Mol. Basel Switz.* 19, 18993–19006.
<https://doi.org/10.3390/molecules191118993>
- Podhorecka, M., Skladanowski, A., Bozko, P., 2010. H2AX Phosphorylation: Its Role in DNA Damage Response and Cancer Therapy. *J. Nucleic Acids* 2010. <https://doi.org/10.4061/2010/920161>
- Porter, A.G., Jänicke, R.U., 1999. Emerging roles of caspase-3 in apoptosis. *Cell Death Differ.* 6, 99–104.
<https://doi.org/10.1038/sj.cdd.4400476>
- Rasul, A., Di, J., Millimouno, F.M., Malhi, M., Tsuji, I., Ali, M., Li, J., Li, X., 2013. Reactive oxygen species mediate isoalantolactone-induced apoptosis in human prostate cancer cells. *Mol. Basel Switz.* 18, 9382–9396. <https://doi.org/10.3390/molecules18089382>
- Sharma, A., Singh, K., Almasan, A., 2012. Histone H2AX phosphorylation: a marker for DNA damage. *Methods Mol. Biol. Clifton NJ* 920, 613–626. https://doi.org/10.1007/978-1-61779-998-3_40
- Sharma, R.A., Gescher, A.J., Steward, W.P., 2005. Curcumin: the story so far. *Eur. J. Cancer Oxf. Engl.* 1990 41, 1955–1968. <https://doi.org/10.1016/j.ejca.2005.05.009>
- Siegel, R.L., Miller, K.D., Jemal, A., 2015. Cancer statistics, 2015. *CA. Cancer J. Clin.* 65, 5–29.
<https://doi.org/10.3322/caac.21254>
- Slater, A.F., Kimland, M., Jiang, S.A., Orrenius, S., 1995. Constitutive nuclear NF kappa B/rel DNA-binding activity of rat thymocytes is increased by stimuli that promote apoptosis, but not inhibited by pyrrolidine dithiocarbamate. *Biochem. J.* 312 (Pt 3), 833–838.
- Thirugnanam, S., Xu, L., Ramaswamy, K., Gnanasekar, M., 2008. Glycyrrhizin induces apoptosis in prostate cancer cell lines DU-145 and LNCaP. *Oncol. Rep.* 20, 1387–1392.
- van Meerloo, J., Kaspers, G.J.L., Cloos, J., 2011. Cell sensitivity assays: the MTT assay. *Methods Mol. Biol. Clifton NJ* 731, 237–245. https://doi.org/10.1007/978-1-61779-080-5_20
- Wang, C., Youle, R.J., 2009. The role of mitochondria in apoptosis*. *Annu. Rev. Genet.* 43, 95–118.
<https://doi.org/10.1146/annurev-genet-102108-134850>
- Wang, L.-H., 2004. Molecular signaling regulating anchorage-independent growth of cancer cells. *Mt. Sinai J. Med. N. Y.* 71, 361–367.

- Wen, J., You, K.-R., Lee, S.-Y., Song, C.-H., Kim, D.-G., 2002. Oxidative stress-mediated apoptosis. The anticancer effect of the sesquiterpene lactone parthenolide. *J. Biol. Chem.* 277, 38954–38964. <https://doi.org/10.1074/jbc.M203842200>
- Yaffe, P.B., Power Coombs, M.R., Doucette, C.D., Walsh, M., Hoskin, D.W., 2015. Piperine, an alkaloid from black pepper, inhibits growth of human colon cancer cells via G1 arrest and apoptosis triggered by endoplasmic reticulum stress. *Mol. Carcinog.* 54, 1070–1085. <https://doi.org/10.1002/mc.22176>
- Yoo, S., Choi, S.Y., You, D., Kim, C.-S., 2016. New drugs in prostate cancer. *Prostate Int.* 4, 37–42. <https://doi.org/10.1016/j.pnil.2016.05.001>
- Zhang, J., Zhu, X., Li, H., Li, B., Sun, L., Xie, T., Zhu, T., Zhou, H., Ye, Z., 2015. Piperine inhibits proliferation of human osteosarcoma cells via G2/M phase arrest and metastasis by suppressing MMP-2/-9 expression. *Int. Immunopharmacol.* 24, 50–58. <https://doi.org/10.1016/j.intimp.2014.11.012>

Fig. 1. Chemical synthesis of PG analogs: DR-P27, DR-P3 and DR-P10.

Fig. 2. Cell viability assay of PG and its derivatives on prostate cancer cells: (A) Derivatives of PG, especially DRP-27, inhibit the proliferation of prostate cancer cells (LNCaP) more effectively than PG as determined by MTT assay. Data shown as mean \pm SD. * $P < 0.05$ compared to control group. (B) Anti-proliferative activity of DRP-27 against LNCaP cells were abrogated by NAC and CI. * $P < 0.001$ compared to control. # $P < 0.01$ compared to DRP-27 treatment group. (C) Morphological changes in LNCaP cells after treatment with DRP-27. Cells were treated for 48 h with various concentrations of DRP-27. Morphological changes were observed using microscopy ($\times 20$ magnification). (D) Cytotoxicity evaluation of DRP-27 on normal prostate cells (RWPE-1) and androgen-independent prostate cancer cells (PC-3 and DU145). Results showed that DRP-27 has minimal toxic effects on RWPE-1 compared to PC-3 and DU145 PCa cells. * $P < 0.05$ compared to RWPE-1 cells. DRP-27 treatment reduces anchorage-independent growth of LNCaP cells: (E) Soft agar assay results show that DRP-27 significantly inhibited the colony formation ability of LNCaP cells. Colonies were detected using crystal violet staining. (F) Quantitative analysis of clonogenesis in LNCaP cells against different concentrations of DRP-27. Data are shown as mean \pm S.D.

Fig. 3. DRP-27 promotes oxidative stress in LNCaP cells: (A) The reactive oxygen species generation was detected by adding 2',7'-dichlorofluorescein diacetate (DCFDA) fluorescent probe and observed by fluorescent microscope. The fluorescent green color indicates generation of reactive oxygen species in DRP-27-treated cells compared to untreated cells. Effect of DRP-27 was abrogated in the presence of anti-oxidant N-acetyl cysteine (NAC). (B) Quantitative analysis of reactive oxygen species generation in LNCaP cells. Data are

shown as mean \pm S.D. *P<0.001 compared to untreated group. #P<0.01 compared to cells treated with 10 μ M DRP-27. DRP-27 induces DNA fragmentation in LNCaP cells: Apoptotic morphological evaluation of LNCaP cells by Hoechst 33258 staining (inverted fluorescence microscopy, \times 20). LNCaP cells were treated with 10 μ M of DRP-27 for 48 h. Arrows show condensed and fragmented nuclei. (C) Control untreated cells do not exhibit condensed and fragmented in nuclei. (D) Treatment with 10 μ M DRP-27 leads to condensed and fragmented nuclei in LNCaP cells. (E) DRP-27 induces apoptosis in LNCaP cells. The cells were cultured and treated with various concentrations of DRP-27 for a period of 48 h. Following incubation, the cells were stained with Annexin FITC (FL1-H) and propidium iodide (FL2-H) and analyzed using flow cytometry. Results indicate that DRP-27 treatment induces potent apoptosis in LNCaP cells.

Fig. 4. DRP-27 activates apoptosis in LNCaP cells. (A) LNCaP cells were treated with various concentrations of DRP-27 (10 and 20 μ M) for 48 h. Cells were stained with Annexin V-FITC (Green) to detect apoptotic cells and PI (Red) to stain the nuclei. Apoptotic activity of DRP-27 was abrogated in the presence of NAC (2.5mM). DRP-27 induces apoptosis in LNCaP cells. (B) LNCaP cells treated with DRP-27 (5 and 10 μ M) for 48 h were stained with TUNEL red to detect apoptotic cells and Hoechst 33342 to stain the nuclei (Blue). (C) Quantitative analysis of TUNEL color intensity produced in LNCaP cells following DRP-27 treatment. Data are shown as mean \pm S.D. *P<0.05 compared to control group. DRP-27 promotes activation of caspase-3 in LNCaP cells. (D) Quantitative analysis of relative levels of caspase-3 by ELISA. Data showed that DRP-27 promotes caspase-3 activation in a dose dependent manner. *P<0.05 compared to control group. (E) Western blot analysis showed that procaspase-3 expression was decreased in DRP-27 treated cells indicating caspase-3 activation. DRP-27 promotes caspase-3 cleavage in LNCaP cells. (F) The cells were cultured and treated with different concentrations of DRP- 27 and probed with cleaved caspase-3 antibody. The confocal microscope pictures indicate that there is an increase in cleaved caspase-3 in DRP-27 treated cells when compared to control. (G) ImageJ analysis showed that cleaved caspase-3 is increased in DRP-27 treated LNCaP cells. *P<0.05 compared to control cells.

Fig. 5. DRP-27 treatment increases the levels of p H_2 AX. LNCaP cells were treated with DRP-27 and subjected to immunofluorescence microscopy probed with anti-p H_2 AX (green

fluorescence) and counter stained with DAPI (blue fluorescence). (A) The level of p_H₂AX was increased in DRP-27 treated LNCaP cells compared to untreated controls. (B) Levels of p_H₂AX were quantitatively measured by using ImageJ software. Data represented as mean ± S.D. *P<0.05 compared to control group.

Fig. 6. DRP-27 targets apoptosis signaling pathways in LNCaP cells. Cells were treated with various concentration of DRP-27 and harvested at 48 h and equal amount of proteins were subjected to SDS-PAGE (12%) and analyzed by Western blot. Results show that DRP-27 upregulates p_H₂AX, and Bax proteins while downregulating the expression of survivin.

Fig. 7. Schematic representation of anti-cancer mechanism of DRP-27 in prostate cancer. DRP-27 induces cell death through reactive oxygen species generation leading to DNA damage and apoptosis.

Accepted manuscript

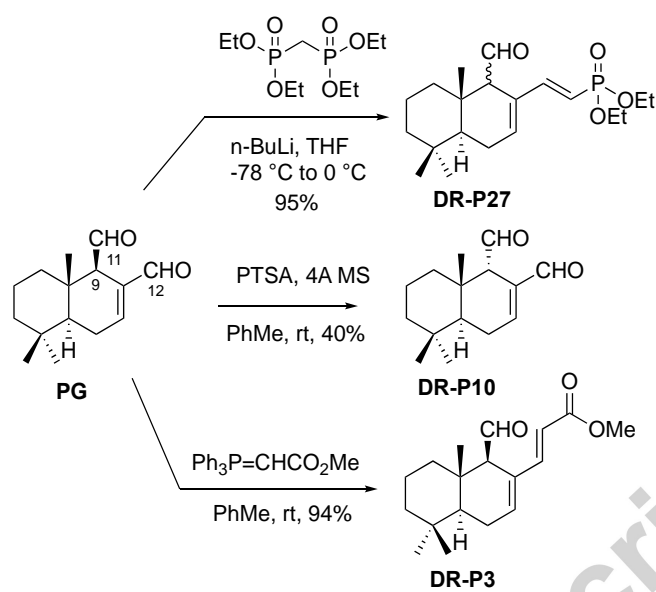


Fig. 1.

(A)

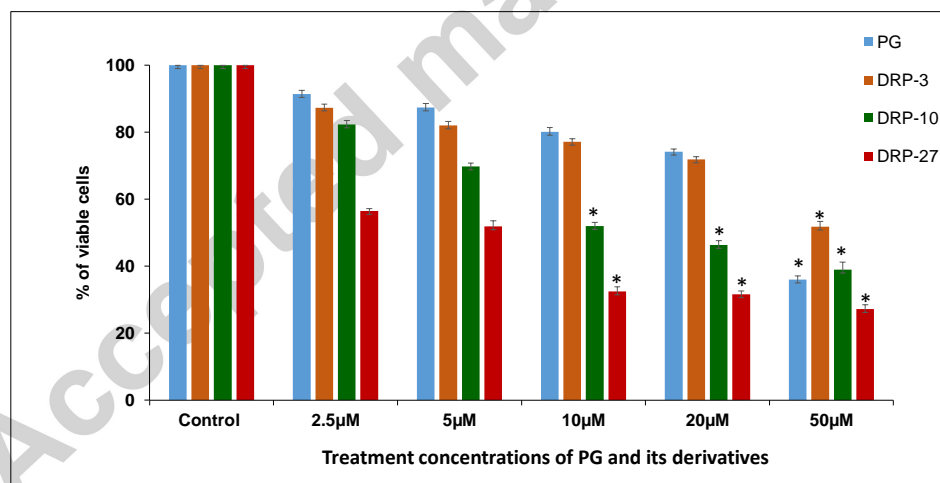


Fig. 2. (A)

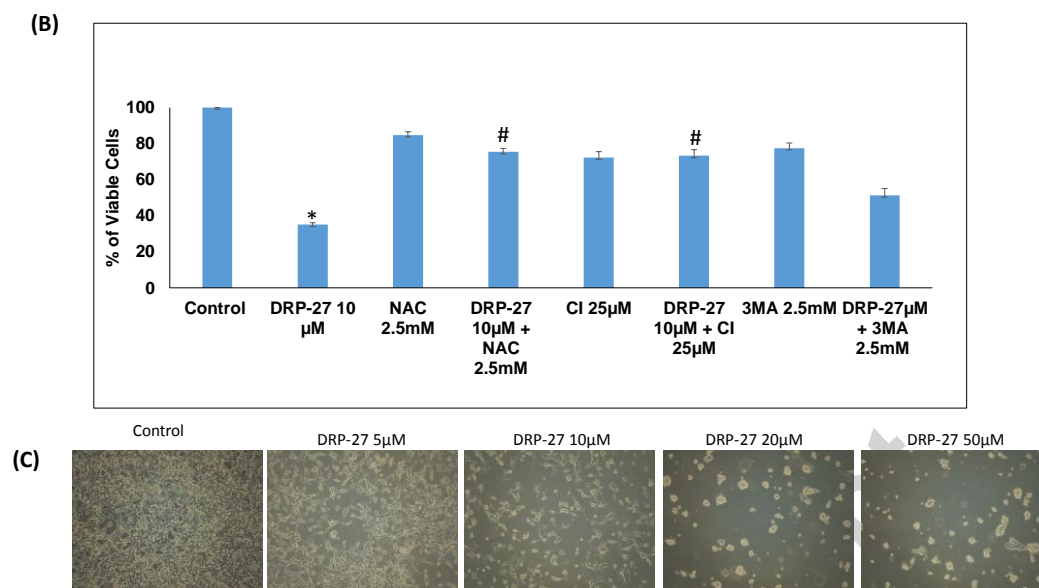


Fig. 2. (B) and (C)

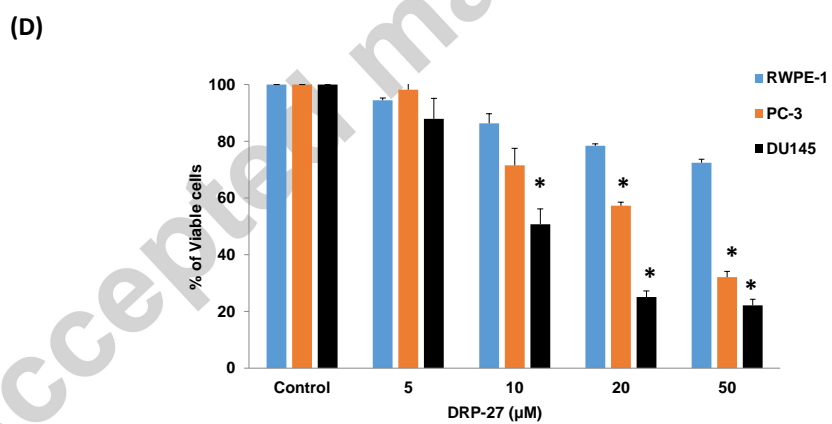


Fig. 2. (D)

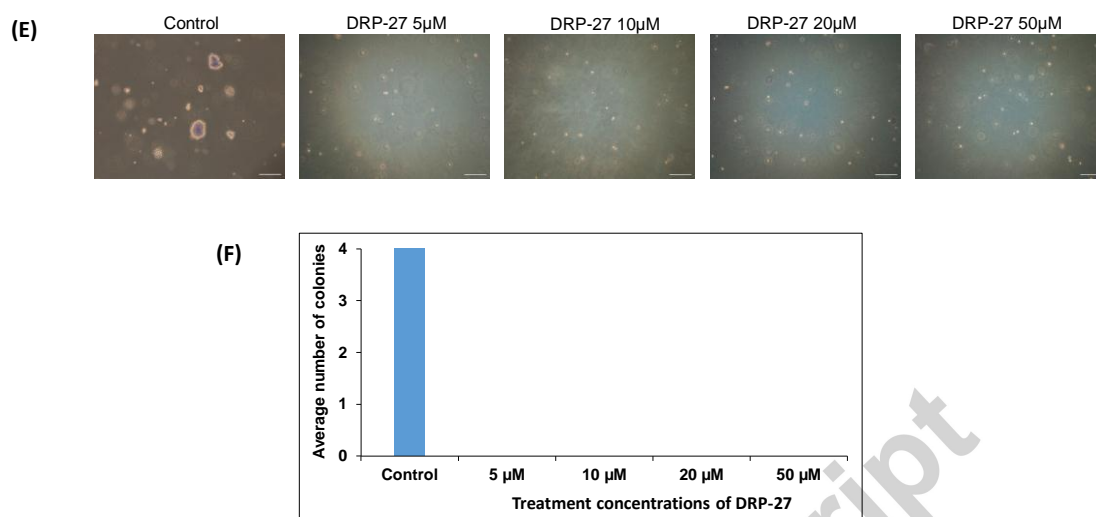


Fig. 2. (E) and (F).

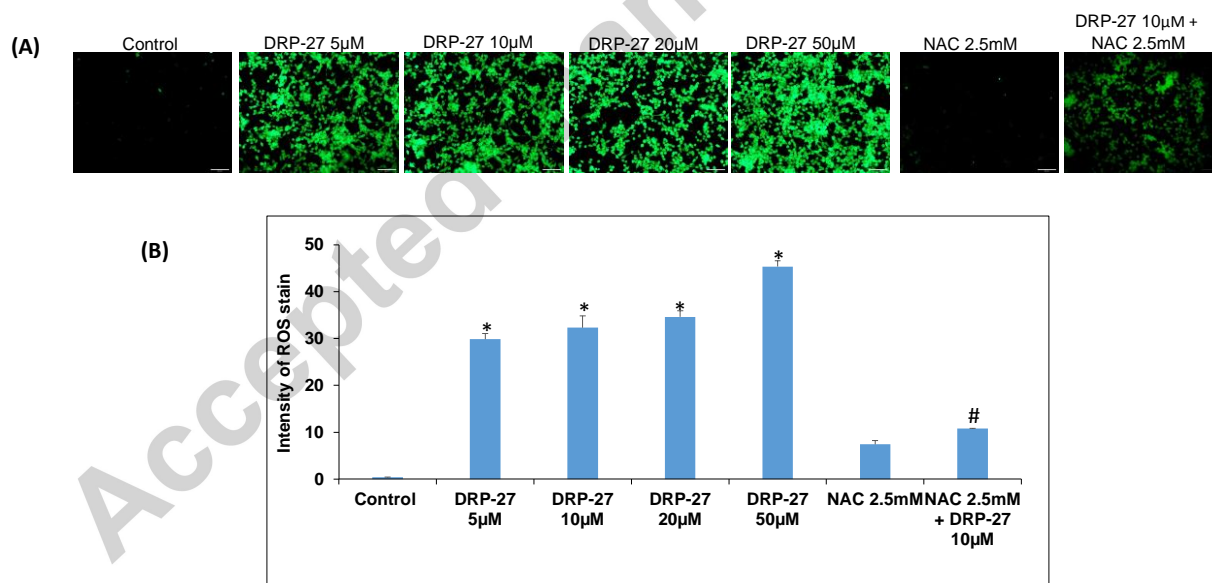


Fig. 3. (A) and (B).

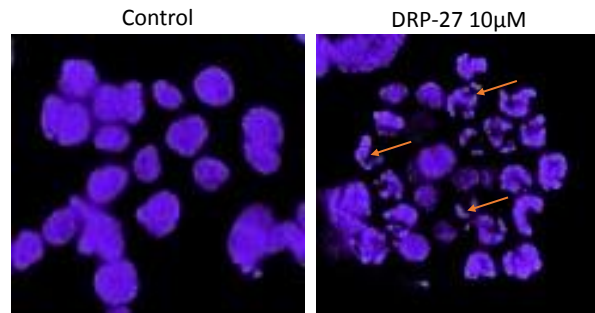


Fig. 3. (C) and (D)

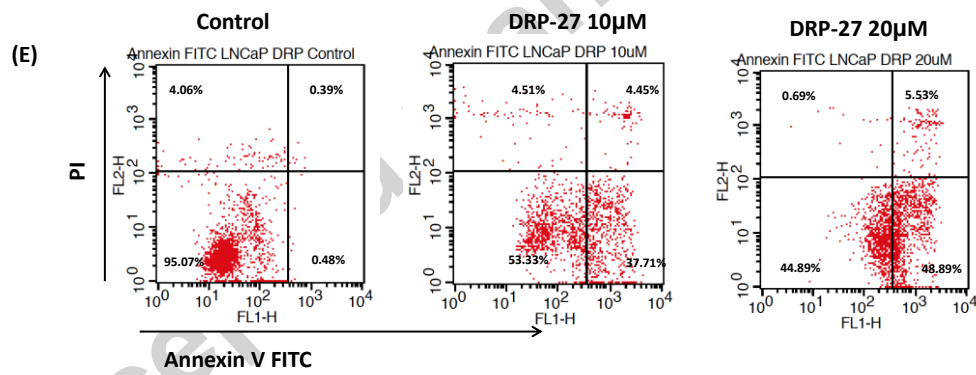


Fig. 3 E.

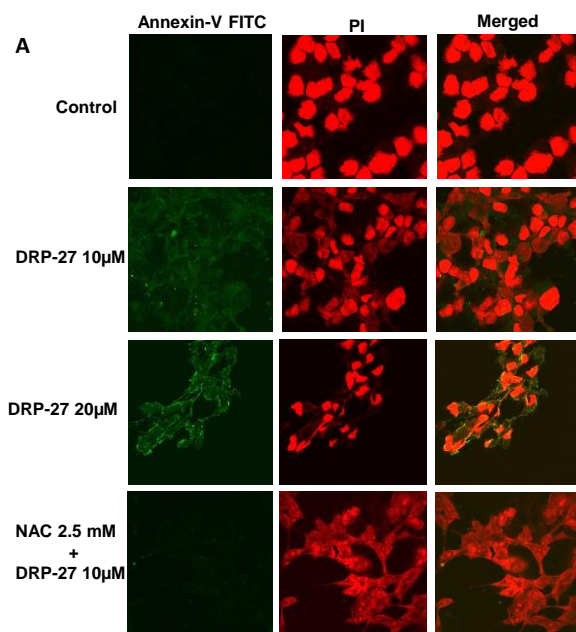
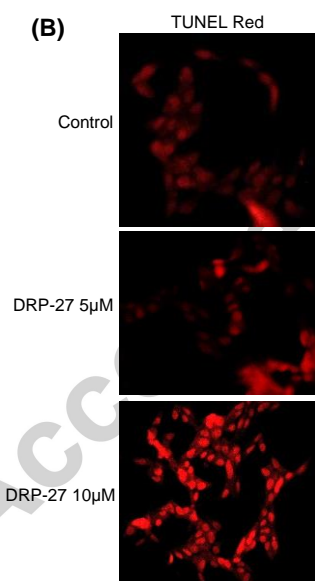


Fig. 4 A.



(C)

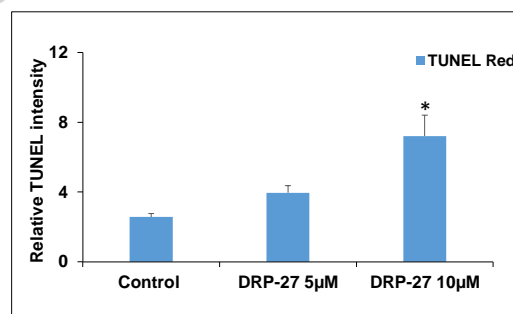


Fig. 4. (B) and (C)

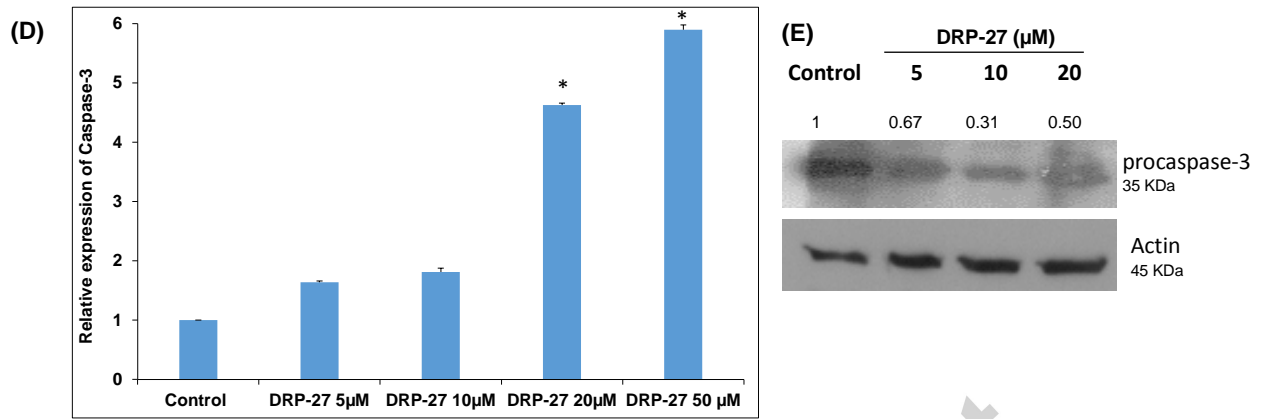


Fig. 4. (D) and (E).

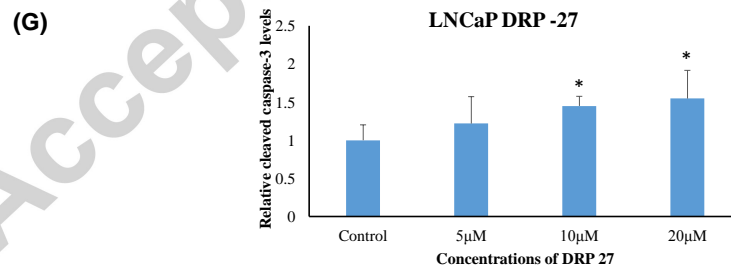
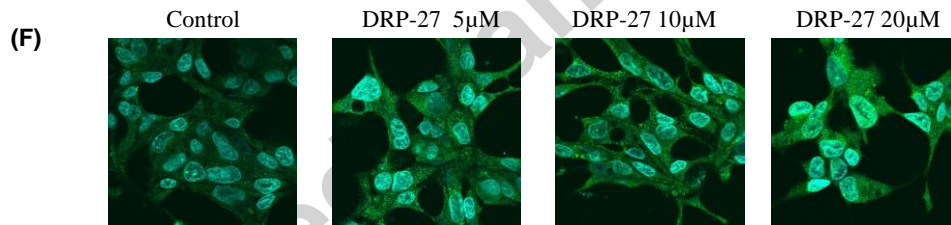


Fig. 4 (F) and (G).

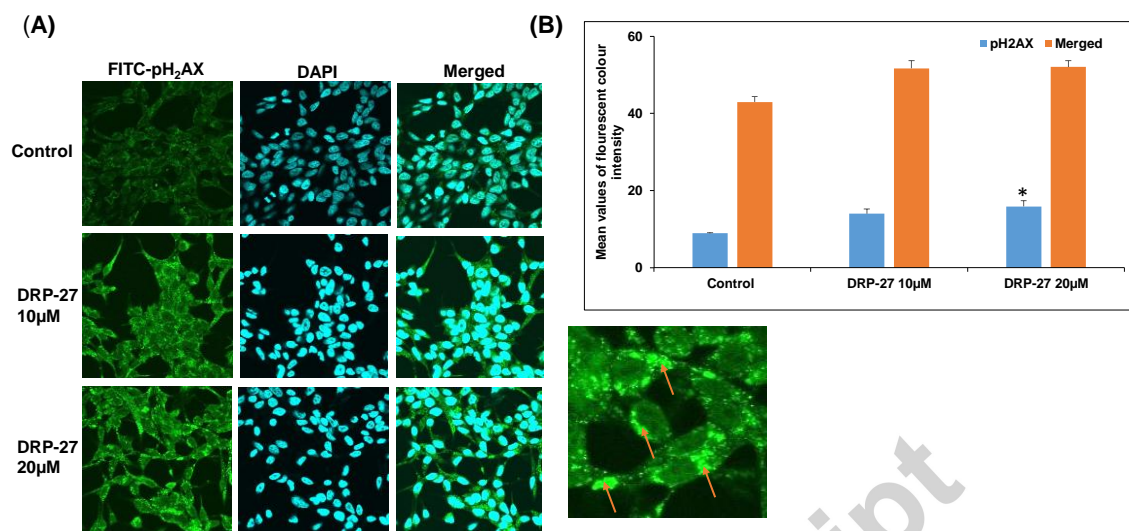


Fig. 5. (A) and (B)

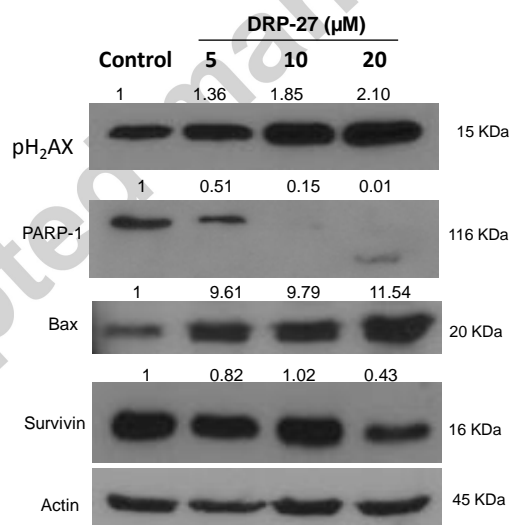


Fig. 6.

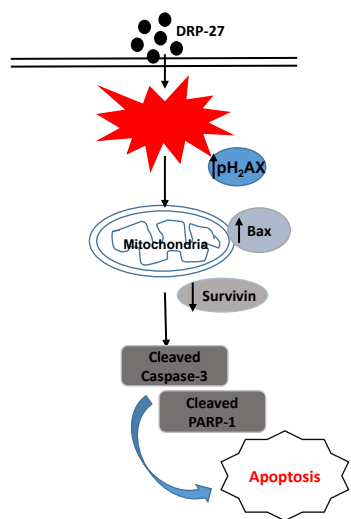


Fig. 7.

Accepted manuscript